Published in final edited form as:
Hypertension. 2014 March ; 63(3): 589–594. doi:10.1161/HYPERTENSIONAHA.113.01171.

Local Effects of Pregnancy on Connexin Proteins that Mediate Ca^{2+}-Associated Uterine Endothelial Nitric Oxide Synthesis

Timothy J. Morschauser[1], **Jayanth Ramadoss**[1,*], **Jill M. Koch**[1], **Fu Xian Yi**[1], **Gladys E. Lopez**[1], **Ian M. Bird**[1,2], and **Ronald R. Magness**[1,2,3]

[1]Department of Ob/Gyn, University of Wisconsin, Madison, WI

[2]Department of Pediatrics, University of Wisconsin, Madison, WI

[3]Department of Animal Sciences, University of Wisconsin, Madison, WI

Abstract

Uterine artery adaptations during gestation facilitate increases in uterine blood flow and fetal growth. Hypothesis: Local expression and distribution of uterine artery connexins play roles in mediating *in vivo* gestational eNOS activation and Nitric Oxide production. We established an ovine model restricting pregnancy to a single uterine horn and measured uterine blood flow, uterine artery shear stress, connexins 37/43 and P^{635}eNOS protein levels in uterine artery and systemic artery [Omental and Renal] endothelium and connexins in vascular smooth muscle. Uterine blood flow and shear stress were locally (unilaterally) and substantially elevated by gestation. During pregnancy uterine artery endothelial gap junction proteins connexins 37/43 were locally regulated in the gravid horn and elevated 10.3- and 25.6-fold; uterine artery endothelial P^{635}eNOS and total eNOS were elevated 3.3- and 2.9-fold; whereas uterine artery vascular smooth muscle connexins 37/43 were locally elevated 12.5- and 5.9-fold, respectively. Less pronounced changes were observed in systemic vasculature except for significant pregnancy-associated increases in omental artery vascular smooth muscle connexin 43 and omental artery endothelial P^{635}eNOS and total eNOS. Gap junction blockade using connexin 43, but not connexin 37 specific GAP peptides abrogated uterine artery endothelial ATP-induced Ca^{2+}-mediated nitric oxide production. Thus uterine artery endothelial connexin43, but not connexin 37 regulates Ca^{2+}-mediated nitric oxide production required for the vasodilation to accommodate increases in uterine blood flow and shear stress during healthy pregnancies.

Keywords

Connexins; Estrogen; Nitric Oxide; Endothelium; Shear Stress; Uterine Blood Flow

Introduction

Pregnancy is characterized by dramatic cardiovascular adaptations, the most substantial being the 30-50 fold increase in the uterine blood flow (UBF) to meet the metabolic demands of developing fetuses [1,2]. Women with endothelial dysfunction have pregnancies with increased susceptibility to preeclampsia[3]. Compared to normal uterine artery (UA) doppler ultrasounds at 23-25 weeks' gestation, preeclamptic women with fetal growth

* Department of Ob/Gyn, UTMB-Galveston. Correspondence: Ronald R. Magness, PhD, Department of Ob/Gyn, Perinatal Research Laboratories, 202 S. Park Street, Madison, WI, 53715 (608) 417-6314 Fax 608-257-1304 rmagness@ wisc.edu.

Conflict(s) of Interest/Disclosure(s)
None

restriction have reduced UBF[4] Pregnant women who exhibit proteinuric hypertension and reductions in UBF also have aberrant levels of circulating estrogens and their metabolites [5] and in some [6,7] but not all studies [8,9] nitric oxide (NO) metabolites.

During the ovarian follicular phase and normal pregnancy, elevations in UBF are associated with higher endogenous estrogen[2, 10] and UA endothelial (UAendo) elevations in estrogen receptors (ER)[11, 12], endothelial nitric oxide synthase (eNOS), and NO[9,13-15,]. Local ER and NO-mediated regulation of UBF was demonstrated by decreases in UBF in response to unilateral infusion of ER antagonist (ICI-182,780) or NOS inhibitor (L-NAME)[10, 16-18]. To better understand local UBF and eNOS regulation, we developed a unilateral model of pregnancy by isolating one uterine horn (nongravid) so that pregnancy is restricted only to the other horn (gravid) throughout gestation[19, 20]. UA endothelial cells from pregnant ewes (P-UAECs)[21] have sustained excitatory eNOS phosphorylation at serine 635 (P^{635}) with ATP treatment, suggesting this site is an important index of eNOS activity[22, 23]. A better understanding of *in vivo* regulation of eNOS activation is important for deciphering gestational regulation of UBF. For instance, the frictional force of flowing blood exerted on the endothelium, shear stress, is a very potent powerful physiologic stimulus of endothelial NO production and needs additional scrutiny in the UAs *in vivo*[24,25]

Emerging literature has defined important interactions between Gap junctions and NO signaling for the development of hypertension[26]. Various connexin isoforms have been reported in, vascular smooth muscle (VSM)[27] and endometrium[28]. C×43, but not C×37 or 40 were detectable in passage 4 P-UAECs and that when C×43 Gap junction channels were blocked with Gap27 (a C×43 specific extracellular loop mimetic peptide), normal pregnancy-associated Ca^{2+} bursts and eNOS activation upon ATP stimulation were abrogated. [29]

We hypothesize that associated with physiologic rises in UBF and UA shear stress, *ex vivo* expressions of UAendo and UAvsm Gap junction proteins are elevated during pregnancy vs. the nonpregnant luteal and follicular phase, and that restricting pregnancy to a single uterine horn only induces local unilateral ipsilateral increases in UBF, UA shear stress, and UAendo/ UAvsm connexin expression. We evaluated: 1) UBF, UA shear stress and expression of C×37/C×43 in UAs (endo vs. VSM) as well as UAendo serine P^{635} and total eNOS during the ovarian cycle and pregnancy; 2) if changes in UBF, shear stress, and expression are unilaterally and locally specific to the gravid uterine vascular bed or also noted in systemic (Omental and Renal) arteries (OA and RA); and 3) if C×37 or C×43 *ex vivo* are functionally responsible for modulating Ca^{2+}-induced NO production by UAendo during gestation.

Materials and Methods

See online supplement (http://hyper.ahajournals.org).

Animal Ethical Approval—We used 54 multiparous ewes (*Ovis Aire*). Protocols were approved by the Animal Care and Use Committee.

Tissue Collection and ex vivo Endothelium vs. VSM Isolation—Nonsurvival surgery was performed on: Nonpregnant (Luteal, n=8; Follicular, n=8), Unilateral Pregnant (Nongravid vs. Gravid sides, n = 15), and Control Pregnant (n=23) groups. Using transonic flow probes bilateral UBF was determined[14] and arteries were obtained and frozen. Endothelial-isolated proteins from UAendo, OAendo, RAendo and adjacent VSM [16] were prepared. Western analysis was performed using antibodies to C×37, C×43, P^{635} eNOS, and total eNOS.

Calculation of Shear Stress—Shear stress was calculated as $4\,Q\eta/\pi r^3$. Q=UBF, η=viscosity and r=radius [25]

Simultaneous in situ measurement of $[Ca^{2+}]i$ and NO in intact UAendo—$[Ca^{2+}]i$ and NO imaging was performed using fura-2 AM and DAF-2 DA[29] comparing control vs. ATP (100uM) treatments with or without (43,37)Gap27 (300 μM) to inhibit C×43 Gap junctions. Additional control (40, 37)Gap26 and scrambled Gap27 were evaluated.

Statistical Analysis—ANOVA was performed (Luteal, Follicular, Nongravid Unilateral, Gravid Unilateral, and Pregnant) followed by comparisons using protected Fisher's Least Significant Difference. Regression analyses were performed to determine the highest order (linear, quadratic, etc. Table S1) regression models between UBF, connexins, and eNOS. Data are reported as Means±SEM ($P<0.05$).

Results

UBF and Shear Stress (Figure 1)

Compared to luteal UBF (21.8±1.4 mL/min), perfusion was elevated to 51.1±5.4 and 42.4±8.9 mL/min during the follicular phase and to the nongravid side of the unilateral pregnant ewes. UBF to unilateral gravid and control pregnant horns were equal (850±74 and 838±68 mL/min) and greater than nonpregnant and unilateral nongravid groups. Compared to luteal (4.1±0.35 dynes/cm^2), follicular phase (8.0±0.85 dynes/cm^2) and unilateral nongravid (6.4±1.76 dynes/cm^2) shear stresses were elevated. Shear stress in both the unilateral gravid and control pregnant groups was equal and significantly elevated (21.5±3.77 and 25.2±1.96 dynes/cm^2).

Connexin 37 and 43 Expression in UAendo and UAvsm

UAendo C×37 remained unchanged and relatively low in follicular and unilateral nongravid groups (2.1±0. 8-and 1.5±0.5-fold of luteal; Figure 2A). UAendo C×37 in the unilateral gravid and control pregnant groups were respectively 6.4±2.0- and 10.3±1.6-fold higher than luteal and greater than follicular and unilateral nongravid groups. UAendo C×43 levels remained unchanged and were relatively low in nonpregnant follicular and unilateral nongravid groups (3.2±0.9- and 5.1±1.0-fold). Unlike C×37, UAendo C43 levels were elevated similarly in the unilateral gravid (21.3±4.1-fold) and control pregnant groups (25.8±4.7-fold). UAendo C×43 was correlated ($P < 0.001$) more so than C×37 with UBF (Figure S-1A/B).

Follicular UAvsm C×37 had intermediary values (2.2±1. 8 fold) compared to either nonpregnant luteal or unilateral nongravid groups (Figure 2B). The unilateral nongravid group was elevated 6.8±2.1-fold. UAvsm C×37 was elevated similarly in the unilateral gravid and control pregnant animals 13.4±2.5-and 12.5±2.2-fold. UAvsm C×43 was elevated in the unilateral nongravid, gravid, and pregnant groups 4.7±1.3-, 5.7±1.1-, and 5.8±1.3-fold, respectively. Follicular UAvsm C×43 had intermediary values (3.2±1.1-fold) similar to the other four groups. UAvsm C×37 was correlated ($P < 0.001$) more so than C×43 with UBF (Figure S-1C/D).

Connexin 37 and 43 Expression in OAendo and RAendo

OAendo C×37, OAendo C×43, and RAendo C×37 remained unchanged (Figure S-2). RAendo C×43 was lower in the unilateral group ($P < 0.012$).

Connexin 37 and 43 Expression in OAvsm and RAvsm

OAvsm C×37 and C×43 were unchanged except C×43 was elevated in pregnant controls (Figure S-3). RAvsm C×37 was decreased in follicular, unilateral, and pregnants. RAvsm C×43 levels were similar amongst the four groups.

P^{635} eNOS and Total eNOS Expression in UAendo, OAendo, and RAendo

Levels of the UAendo excitatory eNOS phosphorylation site P^{635} were relatively low and remained unchanged in the follicular and unilateral nongravids (2.4 ± 0.8-and 1.1 ± 0.4-fold, Figure 3A). UAendo P^{635} eNOS levels were elevated 3.8 ± 0.7-and 3.3 ± 0.6-fold, in the unilateral gravid and pregnant groups, respectively which were greater than unilateral nongravid, but not the folliculars (0.1>P>0.05). UAendo total eNOS for follicular and unilateral nongravids averaged 1.9 ± 0.8- and 0.3 ± 0.1-fold and was equally elevated in unilateral gravid (4.6 ± 1.0-fold) and pregnants (2.9 ± 0.6-fold). UAendo C×37 and C×43 were highly correlated with either UAendo P^{635} eNOS or total eNOS more so in the Unilateral Gravid ($P<0.007$) than the Pregnant Controls (Figure S-4). OAendo P^{635} eNOS remained unchanged in follicular and unilateral groups (1.4 ± 0.4-and 1.1 ± 0.15-fold; Figure 3B), but was elevated 3.0 ± 0.6-fold in pregnant controls. OAendo total eNOS levels remained low in the follicular and unilateral groups (1.9 ± 0.8-and 0.7 ± 0.1-fold) and was elevated 5.8 ± 1.5-fold in pregnant controls. RAendo P^{635} eNOS and total eNOS levels did not change amongst the 4 groups (Figure 3C).

Simultaneous Ex Vivo Imaging of $[Ca^{2+}]i$ and NO in UAendo

To determine the role of Gap junctions on ATP-induced periodic $[Ca^{2+}]i$ bursts and rapid oscillations in UAendo (Figure 4), (43,37)Gap 27[29] was used to interrupt Gap junction communication. Pre-treatment (3h) with (43, 37)Gap 27 had little effect on the ATP-induced maximal $[Ca^{2+}]i$ height or incidence of the initial $[Ca^{2+}]i$ peak, but abrogated long-term $[Ca^{2+}]i$ bursts and oscillation responses. Because (43, 37)Gap 27(sequence SRPTEKTIFII) inhibits C×43 and C×37, we established peptide specificity using (40, 37)Gap 26 (specific to C×40 and C×37; n=5) (Figure 4) or (43, 37 scramble peptide)Gap 27 (n=2) [29]. UAendo (43,37) Gap 27 treatment, not the other peptides, specifically blunted both overall NO production and maximum UAendo NO production rate by 49%.

Discussion

Consistent with previous reports[2,10,16,17], follicular phase and late gestation UBFs were elevated. Restricting pregnancy to a single uterine horn [19, 20] only showed increased ipsilateral UBF possibly due to pregnancy specific uterine adaptations to local endogenous hormone secretion (e.g. estrogen, VEGF, etc). Although there was a 25-50% reduction in total number of placentomes [19], UBF to the gravid unilateral and control pregnant horns was equal as reported in another study [30] in which one horn was ligated on day 5 of pregnancy; however they did not measure nongravid UBF. The mechanism(s) how UBF equilibrates in this unilateral model vs. pregnant controls are important, even more so under the limited uterine tissue available prior to conception. One of the most potent mechanisms for controlling vasodilator production and vascular remodeling is laminar shear stress [24,25,31]. We report the first *in vivo* estimates of ovine UA shear stress showing that it was substantially and equally elevated to the unilateral gravid and in control pregnancy. The pregnancy-induced fold change of UBF was greater than that of shear stress demonstrating that shear stress is normalized during pregnancy, due mainly to the increase in UA radius, but to a lesser extent reductions in viscosity (Supplement)[25]. Shear stress is a very powerful physiologic stimulator of eNOS[25,31] and eNOS P^{635} [32] suggesting that NO produced by UAendo via local/unilateral increases in UA shear stress helps drive increases in UBF.

This is the first report showing that C×37 and C×43 are highly expressed and elevated in UAendo by pregnancy. Previously we did not detect C×37 in cultured P-UAECs and C×43 showed equal expression in nonpregnant (NP)-UAECs and P-UAECs[29]. Thus C×37 expression is lost and C×43 is reduced by the 4th passage in culture. Alternatively the observed UAendo C×37 could be derived from another cell type present in the endothelial-isolated enriched tunica intimal proteins (e.g. pericytes) which were removed during the UAEC isolation processes[15,21]. Consistent with other vascular beds[33] we also noted significant UAvsm expression of C×37 and C×43. UAvsm C×37 and C×43 were elevated by the follicular phase, but even more so by pregnancy; both are physiologic states of high estrogen[2,5,10,12,16]. The unilateral nongravid side also showed elevations in UAvsm C×37 and C×43, demonstrating that systemic circulating hormones (e.g. estrogen) may partly regulate VSM C×s. Myometrial C×43 is up-regulated when endogenous estrogen is elevated and C×43 is categorized as a "contraction associated protein" increased in labor when the estrogen/progesterone ratio is high [34]. Pregnancy-associated C×37 were increased equally in UAendo and UAvsm (10.3-and 12.5-fold) suggesting that C×37 synthesis may be co-regulated for forming myoendothelial Gap junctions between UAendo and UAvsm[27,35]. By contrast, pregnancy-induced C×43 increases were much greater in UAendo than UAvsm (25.5-and 5.8-fold).

Consistent with previous reports [9,11-15], we observed that UAendo total eNOS is elevated during the follicular phase and pregnancy reporting for the first time that surgically- induced unilateral gravid, but not nongravid UAendo had increases in eNOS expression. Stimulatory phosphorylation serine 635, an index of enzyme activity in UAendo[22, 23], is also elevated unilaterally by pregnancy suggesting that both expression capacity and activity of eNOS are increased. Additionally, we observed pregnancy-associated adaptations in the nonreproductive OAendo which showed increases in both P^{635} eNOS and total eNOS, the latter confirming our previous observation[15]. This suggests a systemic OAendo adaptation to a vasorelaxation phenotype consistent with studies demonstrating that systemic and uterine resistance vessels show greater endothelium and NO- mediated vasorelaxation in pregnant vs. nonpregnant rats [36], and women[37].

Using least squares regression analysis we defined significant relationships between UA C×s with UBF, or eNOS. C×37 or C×43 relative to UBF (Figure S-1) data points for pregnant controls and the unilateral gravid sides clustered in very similar patterns. Moreover, UBF was maintained in the unilateral model similar to that observed in the pregnant controls even though overall uterine space and tissue mass were reduced. R^2 values for UAendo C×37 and C× 43 with UBF were 0.48 and 0.60, respectively demonstrating a stronger relationship for UAendo C×43 to regulate UBF. In contrast, UAvsm C×37, not C×43, showed a strong a relationship with UBF; R^2 values of 0.43 and 0.18, respectively, suggesting that UAvsm C×37 may in part be regulating vascular growth and remodeling[2, 38]. Correlations of UAendo C×43 with P^{635} eNOS and total eNOS were highly significant and greater than UAendo C×37 (Figure S-4). Within the gravid unilaterals, this relationship was greatly improved demonstrating that C×43 and eNOS are more correlated with the gravid side of the pregnancy; i.e. R^2 values increased to 0.43 for P^{635} eNOS and 0.47 for total eNOS independent of the substantially lower control pregnant data points. Thus UAendo C×43, but not C×37, has an intimate positive association with P^{635} eNOS and total eNOS. This suggests that UBF maintenance, even in the face of greatly reduced uterine space, is adaptive via an eNOS mechanism to maintain UA delivery of nutrients and oxygen for fetal growth.

The current physiologic functional *ex vivo* data showing that C×43, but not C×37, was a prerequisite requirement for ATP-mediated Ca^{2+} burst associated NO production are consistent with our observations in passage 4 P-UAECs, but not NP-UAECs[29]. Gap27, a

connexin (43, 37) specific peptide, did not alter the initial peak of calcium, but reduced subsequent Ca^{2+} bursts seen upon ATP treatment. As recently described[39] the ATP-stimulated [Ca^{2+}]i response in individual UAendo cells is comprised of an initial peak followed by transient calcium bursts are required for the simultaneous and robust production of NO. We show herein that the ATP-stimulated pregnancy programmed burst pattern for Ca^{2+}-mediated NO production was specifically abrogated by pre-treatment with (43,37)Gap27, but not (40,37)Gap26, or scrambled Gap27. Moreover, (43, 37) Gap27 pretreatment of UAendo from pregnancy converted ATP-stimulated Ca^{2+} and NO responses to ones that were identical to those we previously observed from nonpregnant Luteal or Follicular UAendo [39].

Perspectives

Gap junctions have a role in regulating vasodilatory pathways that modulate numerous cardiovascular functions which when dysfunctional contribute to hypertension. The connection between endothelial dysfunction, reduced NO biosynthesis, and reduced UBF in preeclampsia was previously noted [4,6,7,9] . We show the normal physiologic rises in UBF and UA shear stress, C×43, and eNOS are increased via local mechanisms only in the uterine vessels adjacent to the uterine horn that contain a feto-placental unit. Understanding the mechanisms regulating UA function, gives us greater understanding of the specific mechanisms controlling normal UBF during gestation which may function abnormally in preeclampsia. Mechanisms controlling UBF may be modulated by local steroid hormones or growth factors produced by the placenta, locally secreted into the uterine venous blood and reaching the tissues via arterial-venous shunts or the lymphatic drainage in order to cause unilateral vasodilation and vascular remodeling. We reported that UA endothelial ATP-induced eNOS activation and NO production is Ca^{2+}-mediated and has an obligatory requirement for C×43. Thus even in conditions of uterine space limitations and placental insufficiency, uterine perfusion is partly maintained at control levels via the co-regulation of C×43 and eNOS for more robust NO production. The end result is to maintain UBF for nutrient and oxygen delivery and thus fetal growth in an albeit comprised *in utero* environment.

Supplementary Material

Refer to Web version on PubMed Central for supplementary material.

Acknowledgments

We thank SO Jobe, MB Pastore, MY Sun, TM Phernetton, JL Austin, KM Grindle, and T Taylor. This work was partial fulfillment of TJM's MS degree for the Endocrinology/Reproductive Physiology Training Program.

Funding Sources

NIH HL49210,HL87144,HD38843, HL117341 (RRM),AA19446 (JR),and HL079020 (IMB).

References

1. Duvekot JJ, Peeters LLH. Maternal cardiovascular hemodynamic adaptations to pregnancy. Obstet Gynec Survey. 1994:49.
2. Magness, RR. Maternal cardiovascular and other physiologic responses to the endocrinology of pregnancy. In: Fuller Bazer, HPI., editor. The Endocrinology of Pregnancy. Vol. 18. Totowa NJ: 1998. p. 507-539.Chapter
3. Ness RB, Sibai BM. Shared and disparate components of the pathophysiologies of fetal growth restriction and preeclampsia. Am J Obstet Gynecol. 2006; 195:40–49. [PubMed: 16813742]

4. Zamudio S, Palmer SK, Dahms TE, Berman JC, Young DA, Moore LG. Alterations in uteroplacental blood flow precede hypertension in preeclampsia at high altitude. J Appl Physiol. 1995; 79:15–22. [PubMed: 7559213]
5. Jobe SO, Tyler CT, Magness RR. Aberrant synthesis, metabolism, and plasma ccumulation of circulating estrogens and estrogen metabolites in preeclampsia: Implications for vascular dysfunction. Hypertension. 2013; 61:480–487. [PubMed: 23319542]
6. Davidge ST, Stranko CP, Roberts JM. Urine but not plasma nitric oxide metabolites are decreased in women with preeclampsia. Am J Obstet Gynecol. 1996; 174:1008–1013. [PubMed: 8633627]
7. Seligman SP, Buyon JP, Clancy RM, Young BK, Abramson SB. The role of nitric oxide in the pathogenesis of preeclampsia. Am J Obstet Gynecol. 1994; 171:944–948. [PubMed: 7943106]
8. Conrad KP, Kerchner LJ, Mosher MD. Plasma and 24-h NO(x) and cGMP during normal pregnancy and preeclampsia in women on a reduced NO(x) diet. Am J Physiol. 1999; 277:F48–57. [PubMed: 10409297]
9. Sladek SM, Magness RR, Conrad KP. Nitric oxide and pregnancy. Am J Physiol. 1997; 272:R441–463. [PubMed: 9124465]
10. Gibson TC, Phernetton TM, Wiltbank MC, Magness RR. Development and use of an ovarian synchronization model to study the effects of endogenous estrogen and nitric oxide on uterine blood flow during ovarian cycles in sheep. Biol Reprod. 2004; 70:1886–1894. [PubMed: 14985241]
11. Byers MJ, Zangl A, Phernetton TM, Lopez G, Chen DB, Magness RR. Endothelial vasodilator production by ovine uterine and systemic arteries: Ovarian steroid and pregnancy control of ERα and ERβ levels. J Physiol. 2005; 565:85–99. [PubMed: 15774511]
12. Pastore MB, Jobe SO, Ramadoss J, Magness RR. ER-α and ER-β in the uterine vascular endothelium during pregnancy: Functional implications for regulating uterine blood flow. Semin Reprod Med. 2012; 30:46–61. [PubMed: 22271294]
13. Magness RR, Sullivan JA, Li Y, Phernetton TM, Bird IM. Endothelial vasodilator production by uterine and systemic arteries. VI. Ovarian and pregnancy effects on eNOS and NO(x). Am J Physiol Heart Circ Physiol. 2001; 280:H1692–1698. [PubMed: 11247781]
14. Vagnoni KE, Shaw CE, Phernetton TM, Meglin BM, Bird IM, Magness RR. Endothelial vasodilator production by uterine and systemic arteries. III. Ovarian and estrogen effects on NO synthase. Am J Physiol. 1998; 275:H1845–1856. [PubMed: 9815093]
15. Magness RR, Shaw CE, Phernetton TM, Zheng J, Bird IM. Endothelial vasodilator production by uterine and systemic arteries. II. Pregnancy effects on NO synthase expression. Am J Physiol. 1997; 272:H1730–1740. [PubMed: 9139957]
16. Magness RR, Phernetton TM, Gibson TC, Chen DB. Uterine blood flow responses to ICI 182 780 in ovariectomized oestradiol-17β-treated, intact follicular and pregnant sheep. J Physiol. 2005; 565:71–83. [PubMed: 15774510]
17. Rosenfeld CR, Cox BE, Roy T, Magness RR. Nitric oxide contributes to estrogen- induced vasodilation of the ovine uterine circulation. J Clin Invest. 1996; 98:2158–2166. [PubMed: 8903336]
18. Miller SL, Jenkin G, Walker DW. Effect of nitric oxide synthase inhibition on the uterine vasculature of the late-pregnant ewe. Am J Obstet Gynecol. 1999; 180:1138–1145. [PubMed: 10329868]
19. Meyer KM, Koch JM, Ramadoss J, Kling PJ, Magness RR. Ovine surgical model of uterine space restriction: Interactive effects of uterine anomalies and multifetal gestations on fetal and placental growth. Biol Reprod. 2010; 83:799–806. [PubMed: 20574052]
20. Sun MY, Habeck JM, Meyer KM, Koch JM, Ramadoss J, Blohowiak SE, Magness RR, Kling PJ. Ovine uterine space restriction alters placental transferrin receptor and fetal iron status during late pregnancy. Pediatr Res. 2013; 73:277–285. [PubMed: 23202722]
21. Bird IM, Sullivan JA, Di T, Cale JM, Zhang L, Zheng J, Magness RR. Pregnancy- dependent changes in cell signaling underlie changes in differential control of vasodilator production in uterine artery endothelial cells. Endocrinology. 2000; 141:1107–111. [PubMed: 10698187]
22. Ramadoss J, Pastore MB, Magness RR. Endothelial caveolar subcellular domain regulation of endothelial nitric oxide synthase. Clin Exper Pharm Physiol. 2013; 40:753–764.

23. Ramadoss J, Liao WX, Morschauser TJ, Lopez GE, Patankar MS, Chen DB, Magness RR. Endothelial caveolar hub regulation of adenosine triphosphate-induced endothelial nitric oxide synthase subcellular partitioning and domain-specific phosphorylation. Hypertension. 2012; 59:1052–1059. [PubMed: 22454479]
24. Noris M, Morigi M, Donadelli R, Aiello S, Foppolo M, Todeschini M, Orisio S, Remuzzi G, Remuzzi A. Nitric oxide synthesis by cultured endothelial cells is modulated by flow conditions. Circ Res. 1995; 76:536–543. [PubMed: 7534657]
25. Sprague B, Chesler NC, Magness RR. Shear stress regulation of nitric oxide production in uterine and placental artery endothelial cells: Experimental studies and hemodynamic models of shear stresses on endothelial cells. Int J Dev Biol. 2010; 54:331–339. [PubMed: 19876820]
26. Looft-Wilson RC, Billaud M, Johnstone SR, Straub AC, Isakson BE. Interaction between nitric oxide signaling and gap junctions: Effects on vascular function. Biochim Biophys Acta. 2012; 1818:1895–1902. [PubMed: 21835160]
27. Billaud M, Marthan R, Savineau JP, Guibert C. Vascular smooth muscle modulates endothelial control of vasoreactivity via reactive oxygen species production through myoendothelial communications. PLoS One. 2009; 4:e6432. [PubMed: 19649279]
28. Granot I, Dekel N, Bechor E, Segal I, Fieldust S, Barash A. Temporal analysis of connexin43 protein and gene expression throughout the menstrual cycle in human endometrium. Fertil Steril. 2000; 73:381–386. [PubMed: 10685547]
29. Yi FX, Boeldt DS, Gifford SM, Sullivan JA, Grummer MA, Magness RR, Bird IM. Pregnancy enhances sustained CA2+ bursts and endothelial nitric oxide synthase activation in ovine uterine artery endothelial cells through increased connexin 43 function. Biol Reprod. 2010; 82:66–75. [PubMed: 19741206]
30. Caton D, Pendergast JF, Bazer FW. Uterine blood flow: Periodic fluctuations of its rate during pregnancy. Am J Physiol. 1983; 245:R850–852. [PubMed: 6660331]
31. Kuchan MJ, Frangos JA. Role of calcium and calmodulin in flow-induced nitric oxide production in endothelial cells. Am J Physiol. 1994; 266:C628–636. [PubMed: 8166225]
32. Corson MA, James NL, Latta SE, Nerem RM, Berk BC, Harrison DG. Phosphorylation of endothelial nitric oxide synthase in response to fluid shear stress. Circ Res. 1996; 79:984–991. [PubMed: 8888690]
33. Li X, Simard JM. Multiple connexins form gap junction channels in rat basilar artery smooth muscle cells. Circ Res. 1999; 84:1277–1284. [PubMed: 10364565]
34. Lye SJ, Nicholson BJ, Mascarenhas M, MacKenzie L, Petrocelli T. Increased expression of connexin-43 in the rat myometrium during labor is associated with an increase in the plasma estrogen:Progesterone ratio. Endocrinology. 1993; 132:2380–2386. [PubMed: 8389279]
35. Coleman HA, Tare M, Parkington HC. Endothelial potassium channels, endothelium- dependent hyperpolarization and the regulation of vascular tone in health and disease. Clin Exp Pharmacol Physiol. 2004; 31:641–649. [PubMed: 15479173]
36. Conrad KP, Joffe GM, Kruszyna H, Kruszyna R, Rochelle LG, Smith RP, Chavez JE, Mosher MD. Identification of increased nitric oxide biosynthesis during pregnancy in rats. FASEB J. 1993; 7:566–571. [PubMed: 7682524]
37. Nelson SH, Steinsland OS, Johnson RL, Suresh MS, Gifford A, Ehardt JS. Pregnancy- induced alterations of neurogenic constriction and dilation of human uterine artery. Am J Physiol. 1995; 268:H1694–1701. [PubMed: 7733373]
38. Osol G, Mandala M. Maternal uterine vascular remodeling during pregnancy. Physiology (Bethesda). 2009; 24:58–71. [PubMed: 19196652]
39. Yi FX, Boeldt DS, Magness RR, Bird IM. [Ca2+]i signaling vs. eNOS expression as determinants of NO output in uterine artery endothelium: Relative roles in pregnancy adaptation and reversal by VEGF165. Am J Physiol Heart Circ Physiol. 2011; 300:H1182–1193. [PubMed: 21239633]

Novelty and Significance

What is New?

The Gap junction protein, C×43, is crucial for local Ca^{2+}-mediated eNOS activation and NO production by UA endothelium. We demonstrated an important physiologic mechanistic role for connexins and elevations in UA shear stress to maintain uterine perfusion via NO during pregnancy.

What is Relevant?

Preeclampsia with IUGR is a disorder of pregnancy seen in 5-13% of gestations and is associated with reduced UBF causing significant maternal and fetal morbidity and mortality as well as greater susceptibility and earlier onset of future cardiovascular disease in both the mother and baby.

Summary

In gravid uterine endothelium, we demonstrated that UA shear stress, endothelial C×43 and eNOS are locally elevated and that the gap junction protein C×43 is crucial for Ca^{2+}-mediated eNOS activation. These data demonstrate an important physiologic mechanistic role for connexins in regulating the increases in ovine UBF during pregnancy that is needed for fetal development.

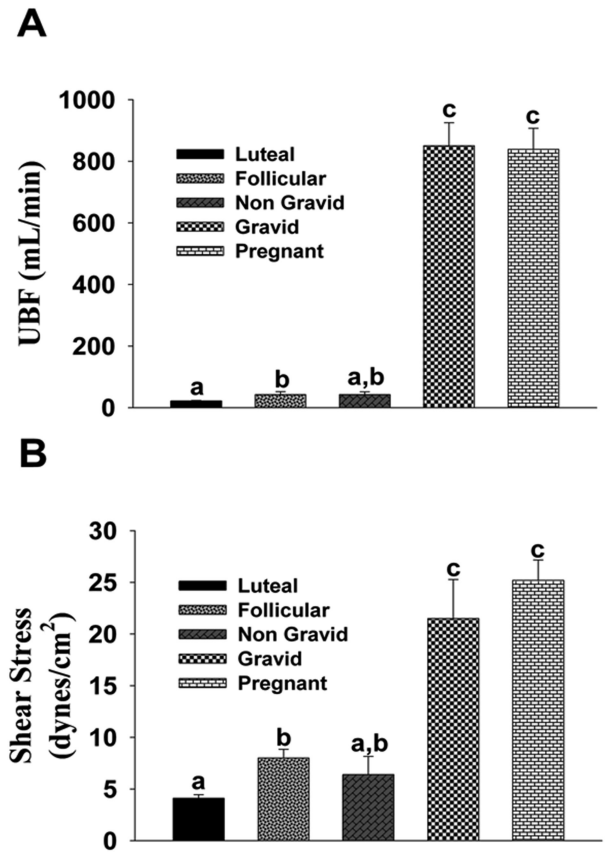

Figure 1. *In Vivo* measurement of uterine artery (A)Blood Flow (UBF) and (B)Shear Stress
Nonpregnant (Luteal and Follicular) and Nongravid/Gravid Unilateral and Pregnant groups. Means±SEM; Different letters denote differences ($P<0.05$).

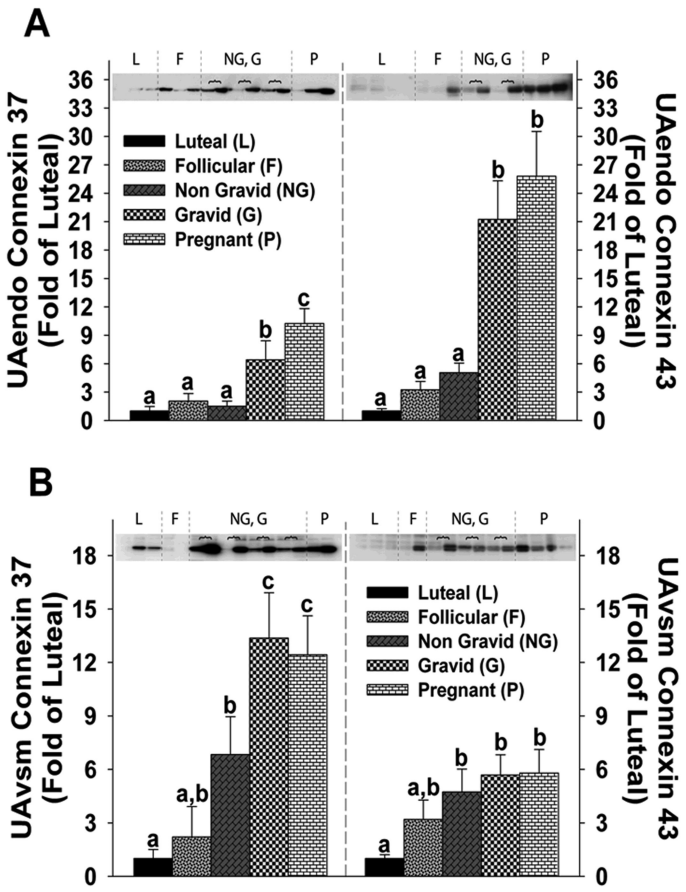

Figure 2. Connexin 37 and 43 protein expression in (A)uterine artery endothelium (UAendo) and (B)vascular smooth muscle (UAvsm) from luteal, follicular, nongravid/gravid unilateral pregnant, and control pregnant ewes

Western Blot analysis comparing relative levels of connexin 37 and 43 in from luteal (L;n=8), follicular (F;n=8), unilateral [nongravid (NG) vs. gravid (G);n=15], and pregnant (P;n=23) sheep. Horizontal brackets represent NG (left),G (right) pairs within individual animals. Data are expressed as Means±SEM fold of L. Different letters denote differences ($P<0.05$).

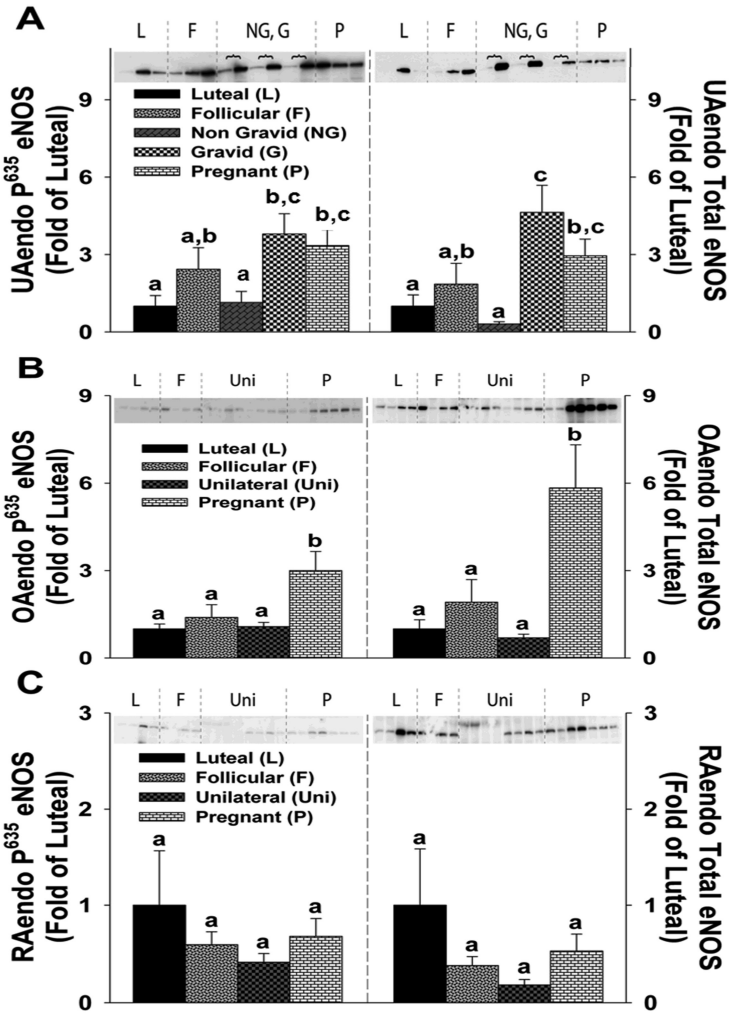

Figure 3. P^{635} eNOS and Total eNOS protein expression in (A)uterine artery (UAendo) and (B&C)systemic artery endothelium (OAendo/RAendo) from luteal, follicular, unilateral, and pregnant ewes

Western Blot analysis comparing the relative levels of P^{635} eNOS and total eNOS in (A)UAendo and (B)OAendo and (C)RAendo obtained from luteal (L;n=8), follicular (F;n=8), unilateral [nongravid (NG) vs. gravid(G) n=15], and pregnant (P;n=23) sheep for UAendo as well as luteal (L;n=4), follicular (F;n=4), unilateral (Uni;n=8) and pregnant (P;n=7) for both OAendo and RAendo. Data are expressed as Means±SEM fold of L. Horizontal brackets ( ) represent NG (left lanes), G(right lanes) pairs within individual animals. Different letters denote differences ($P<0.05$).

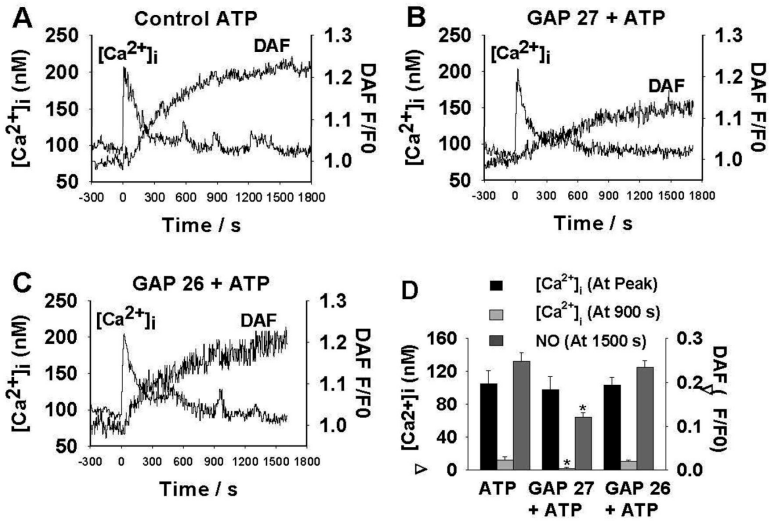

Figure 4. Simultaneous *in situ* measurements of intracellular free Ca^{2+} concentrations ($[Ca^{2+}]i$) and nitric oxide (NO) levels in individual cells of intact uterine artery (UA) endothelium

(A)Representative simultaneous recordings of ATP-induced (100 μM;25 min) increases in $[Ca^{2+}]i$ and DAF-2 fluorescence (NO) from a single intact UAendothelial cell from control pregnant ewes. (B)Effect of Gap27(300 μM) pre-exposure on ATP-induced $[Ca^{2+}]i$ and NO production. (C)Effect of Gap26 (300 μM) pre-exposure on ATP-induced $[Ca^{2+}]i$ and NO production. 4A& C show multiple $[Ca^{2+}]i$ peaks (bursts) whereas 4B shows a single initial $[Ca^{2+}]i$ peak (burst) and reduced NO. (D)Summary: Effect of Gap27 and GAP26(300 μM) pre-treatment on Mean±SEM ATP-induced $[Ca^{2+}]i$ and NO production in intact UAendothelium. Responses: We determined $[Ca^{2+}]i$ at both the initial peak and at 900 s and DAF-2 signals at 1,500 s from 6 to 8 ewes for GAP27 and 5 for GAP26. **P*<0.05 ATP >Gap 27+ATP.